

Article

# Effects of Matte Grade on the Distribution of Minor Elements (Pb, Zn, As, Sb, and Bi) in the Bottom Blown Copper Smelting Process

Qinmeng Wang <sup>1</sup> , Xueyi Guo <sup>2,\*</sup>, Qinghua Tian <sup>2,\*</sup>, Tao Jiang <sup>1</sup>, Mao Chen <sup>3</sup> and Baojun Zhao <sup>3</sup>

<sup>1</sup> School of Minerals Processing and Bioengineering, Central South University, Changsha 410083, China; qmwang@csu.edu.cn (Q.W.); jiangtao@csu.edu.cn (T.J.)

<sup>2</sup> School of Metallurgy and Environment, Central South University, Changsha 410083, China

<sup>3</sup> School of Chemical Engineering, University of Queensland, Brisbane, QLD 4702, Australia; mao.chen@uq.edu.au (M.C.); baojun@uq.edu.au (B.Z.)

\* Correspondence: xyguo@csu.edu.cn (X.G.); qinghua@csu.edu.cn (Q.T.); Tel./Fax: +86-731-8887-6255 (X.G.); +86-731-8887-7863 (Q.T.)

Received: 19 September 2017; Accepted: 9 November 2017; Published: 14 November 2017

**Abstract:** With increasing impurity contents in concentrates, the control of the minor elements is an important issue for the oxygen bottom blown copper smelting process (Shuikoushan process or SKS process). In this work, the distribution behaviors of the minor elements (such as Pb, Zn, As, Sb, and Bi) among the matte, slag, and gas phases as a function of matte grades was investigated by adjusting the ratios of oxygen/ore in the SKS process. With a matte grade around 70%, about 82% As and 70% Bi enters the gas phase, and about 70% Sb and 64% Zn reports to the slag phase, while 55% lead enters the matte phase. The tendency of changes in the distribution of the minor elements in the SKS process is different from that in the Isasmelt process and the Flash smelting process. It may be concluded from this study that the distributions of the minor elements could be optimized to reduce adverse effects in the SKS process by regulating the matte grade.

**Keywords:** element distribution; removing impurity; oxygen bottom blown copper smelting process; SKS process

## 1. Introduction

Copper is considered to be one of the important metals, and it is widely used in electronics, machinery, construction, national defense, and other fields. China has been the largest producer of copper for 12 years, and more than 8,440,000 tons of copper metal was produced in China in 2016. Most copper is produced by the pyrometallurgical processes. The oxygen bottom blown copper smelting process is a newly developed intensified smelting process, which has been widely applied in copper production in China in the past 10 years [1,2]. This process was first industrially tested in the Shuikoushan (SKS) smelter in 1990 and was named originally as the “SKS process”, which is now also referred to as BBS (bottom blown smelting) or BBF (bottom blown furnace). What is more, the SKS process has been also applied to lead [3,4] and antimony [5] productions. In China, the first commercial oxygen bottom blown copper smelting furnace was installed and commercially operated at Fangyuan Nonferrous Metals Co., Ltd. (Dongying, China) in 2008 with an initial design capacity of 50,000 t/a cathode copper, which was expended to 100,000 t/a cathode copper in 2010. Then the technology came into a rapid development stage, and has since been successfully applied in Hengbang Smelter (Yantai, China), Huading Smelter (NeiMonggol, China), Yuguang Smelter (Jiyuan, China), Zhongyuan Gold Smelter (Sanmenxia, China), Minmetals Copper Smelter (Hengyang, China), etc. The typical SKS processes conducted in China are shown in Figure 1. Currently, the process

is also employed in Chile, Peru, Vietnam, Mongolia, and Russia. With the development of bottom blown technology, the oxygen-enriched bottom blowing copper continuous converting process has been developed and commercially applied in Dongying Fangyuan II Smelter [6] and Henan Yuguang Smelter, respectively [7], and the process schematic diagram is shown in Figure 2. The design capacity of the Dongying Fangyuan II Smelter deals with 1,500,000 tons of copper concentrates per year, representing the biggest oxygen bottom blown copper continuous converting plant in China.

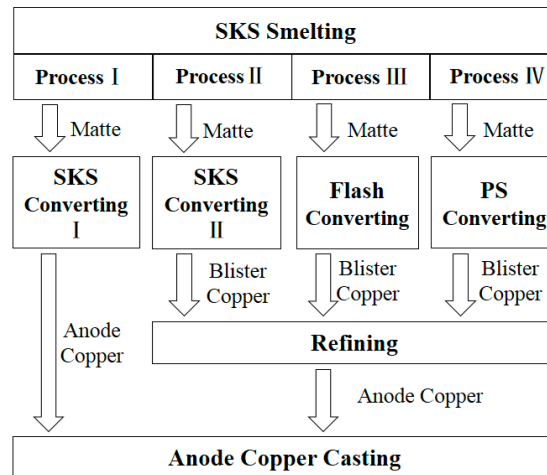


Figure 1. Four typical SKS (Shuikoushan) processes in China.

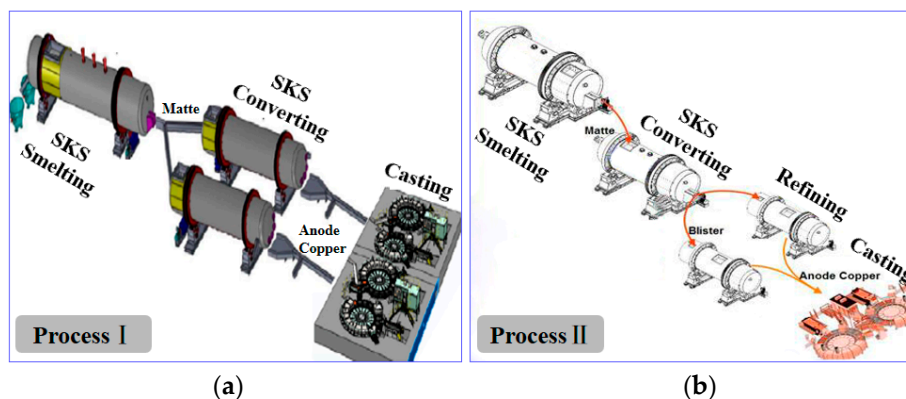


Figure 2. Schematic diagram of SKS smelting and converting process: (a) Fangyuan continuous converting process; (b) Yuguang continuous converting process.

As the SKS process has been widely applied, fundamental research related to the SKS process is required urgently. Chen et al. [8] studied the slag chemistry of the bottom blown copper smelting furnace at Dongying Fangyuan, and analyzed the copper losses in the industrial smelting slags. Shui et al. [9,10] studied the bath surface wave and mixing phenomena in the bottom blown copper smelting furnace, and provided a better understanding of the blowing patterns. Liu et al. [11,12] studied the phase equilibria of the ZnO–FeO–SiO<sub>2</sub> system and ZnO–FeO–SiO<sub>2</sub>–Al<sub>2</sub>O<sub>3</sub> system at P<sub>O<sub>2</sub></sub> 10<sup>−8</sup> atm (10<sup>−3</sup> Pa), which is close to the SKS smelting condition, and found that the presence of ZnO or Al<sub>2</sub>O<sub>3</sub> in the slag significantly increased the liquidus temperature. Zhang et al. [13] analyzed the gas-liquid multi-phase flows in an SKS furnace to optimize the oxygen tuyère structure parameters in the CFD (Computational Fluid Dynamics) method. Yan et al. [14] studied the influences of lance arrangements on the SKS process, and found the optimal lance inclination angle and spacing distance. Guo et al. [15,16] studied the mechanism, multiphase interface behavior, and optimization of the SKS process.

The SKS smelting furnace, which is key to the SKS process, is a horizontal cylindrical reactor similar to the Noranda furnace or the Teniente furnace [1]. However, they still exhibit some differences in furnace structure, process characteristics, and operation parameters. These differences lead to different distributions of oxygen partial pressure in the furnace, and further affect the degree of deviation from equilibrium in different smelting furnaces. Therefore, the distribution behaviors of impurity elements in different smelting furnaces are also different.

However, with increasing impurity contents in the concentrates, the controls of minor elements are important issues for all copper smelters. To date, no work on the distribution of the minor elements in the SKS process has been reported. In this work, the distribution behaviors of the minor elements (such as Pb, Zn, As, Sb, and Bi) among the matte, slag, and gas phases as a function of matte grades in the SKS process is investigated. This work is part of a comprehensive research program to gain a deeper understanding of this new technology.

## 2. Method

### 2.1. Research Methodology

The study of the distributions of the minor elements in the SKS process was carried out by the SKSSIM simulation software (version 1.0, Central South University, Changsha, China) [1,17], combined with actual production data from Dongying Fangyuan Nonferrous Metals Co., Ltd. (Dongying, China).

SKSSIM is an efficient simulation software for the SKS process [17], which is based on the SKS smelting mechanism and the theory of Gibbs free energy minimization. SKSSIM has been successfully used in the actual production in Dongying Fangyuan Nonferrous Metals Co., Ltd. (Dongying, China) and Minmetals Copper (Hunan) Co., Ltd. (Hengyang, China). Therefore, SKSSIM is a convenient way to study the effects of process variables on the distributions of the minor elements. In the present study, the calculations were carried out to study the effects of matte grades on the distribution of the minor elements by adjusting the ratios of oxygen/ore using SKSSIM software. The chemical components in the matte, slag, and gas phases are listed in Table 1.

**Table 1.** Chemical components in the SKS (Shuikoushan) copper smelting process.

Phases	Chemical Components
Gas	SO <sub>2</sub> , SO <sub>3</sub> , S <sub>2</sub> , O <sub>2</sub> , N <sub>2</sub> , H <sub>2</sub> O, PbO, PbS, Zn, ZnS, As <sub>2</sub> , AsO, AsS, SbO, SbS, BiS
Slag	FeO, Cu <sub>2</sub> S, Cu <sub>2</sub> O, Fe <sub>3</sub> O <sub>4</sub> , FeS, PbO, ZnO, As <sub>2</sub> O <sub>3</sub> , Sb <sub>2</sub> O <sub>3</sub> , Bi <sub>2</sub> O <sub>3</sub> , SiO <sub>2</sub> , CaO, MgO, Al <sub>2</sub> O <sub>3</sub>
Matte	Cu <sub>2</sub> S, Cu, FeS, FeO, Fe <sub>3</sub> O <sub>4</sub> , Pb, PbS, ZnS, As, Sb, Bi

The SKS system is approximated under isothermal and isobaric airtight conditions. The smelting temperature used in the calculation is fixed at 1473 K (1200°C). The activity coefficient of each component is selected from the literature [18–21] and listed in Table 2, which are crucial in the SKS process multiphase equilibrium calculation. The standard Gibbs free energy of each component formation is listed in Table 3 [18–21].

**Table 2.** Activity coefficient in the SKS process.

Components	Phase	Activity Coefficient
Cu <sub>2</sub> S	Matte	1
FeS	Matte	$0.925/(N_{Cu_2S} + 1)$
Cu	Matte	14
FeO	Matte	$exp[5.1 + 6.2(\ln N_{Cu_2S}) + 6.41(\ln N_{Cu_2S})^2 + 2.8(\ln N_{Cu_2S})^3]$
Fe <sub>3</sub> O <sub>4</sub>	Matte	$exp[4.96 + 9.9(\ln N_{Cu_2S}) + 7.43(\ln N_{Cu_2S})^2 + 2.55(\ln N_{Cu_2S})^3]$
Pb	Matte	23
PbS	Matte	$exp[-2.716 + 2441/T + (0.815 - 3610/T)(80 - [Pct \cdot Cu]_{mt})/100]$
ZnS	Matte	$exp[-2.054 + 6917/T - (1.522 - 1032/T)(80 - [Pct \cdot Cu]_{mt})/100]$
As	Matte	$8.087 - 0.128[Pct \cdot Cu]_{mt} + 0.014[Pct \cdot Cu]_{mt} \times \lg[Pct \cdot Cu]_{mt}$
Sb	Matte	$-0.996 + 2.42[Pct \cdot Cu]_{mt} - 1.26[Pct \cdot Cu]_{mt} \times \lg[Pct \cdot Cu]_{mt}$
Bi	Matte	$10^{(1900/T - 0.464)}$
FeO	Slag	$1.42N_{FeO} - 0.044$
SiO <sub>2</sub>	Slag	2.1
Fe <sub>3</sub> O <sub>4</sub>	Slag	$0.69 + 56.8N_{Fe_3O_4} + 5.45N_{SiO_2}$
Cu <sub>2</sub> O	Slag	$57.14N_{Cu_2O}$
FeS	Slag	70
Cu <sub>2</sub> S	Slag	$exp(2.46 + 6.22N_{Cu_2S})$
PbO	Slag	$exp(-3330/T)$
ZnO	Slag	$exp(920/T)$
As <sub>2</sub> O <sub>3</sub>	Slag	$3.838exp(1523/T) \times P_{O_2}^{0.158}$
Sb <sub>2</sub> O <sub>3</sub>	Slag	$exp(1055.66/T)$
Bi <sub>2</sub> O <sub>3</sub>	Slag	$exp(-1055.66/T)$

**Table 3.** Standard Gibbs free energy (J·mol<sup>-1</sup>) of the formation of each component.

Components	State	A <sub>ij</sub>	B <sub>ij</sub>
Cu <sub>2</sub> S	liquid	-145,349	43.06
FeS	liquid	-135,556	43.06
PbS	liquid	-151,881	79.67
ZnS	solid	-391,434	203.08
Cu <sub>2</sub> O	liquid	-137,139	54.25
FeO	liquid	-259,244	62.38
Fe <sub>3</sub> O <sub>4</sub>	solid	-1,097,693.74	305.93
As <sub>2</sub> O <sub>3</sub>	liquid	-1,215,325.18	457.37
Sb <sub>2</sub> O <sub>3</sub>	liquid	-687,438	237.86
Bi <sub>2</sub> O <sub>3</sub>	liquid	-563,470	257.66
PbO	liquid	-196,818	79.15
ZnO	solid	-475,260	208.63
SiO <sub>2</sub>	liquid	-912,677	180.92
SO <sub>3</sub>	gas	-459,543	165.15
SO <sub>2</sub>	gas	-361,500	72.49
As <sub>2</sub>	gas	-415,418	113.24
AsS	gas	-184,465	45.88
AsO	gas	-257,759	46.12
SbO	gas	-126,601	-60.35
SbS	gas	103,194	-59.91
BiS	gas	-0.057	96.74
PbO	gas	60,860	-54.39
PbS	gas	57,812	-53.83
ZnS	gas	13,200	32.15

## 2.2. Verification of SKSSIM

The industrial data on compositions of the mixed concentrates and operation parameters under stable operation conditions were taken from Dongying Fangyuan Nonferrous Metals Co., Ltd. (Dongying, China), and are listed in Tables 4 and 5.

**Table 4.** Composition of the mixed concentrate in the furnace.

Component	Cu	Fe	S	Pb	Zn	As	Sb	Bi	SiO <sub>2</sub>	MgO	CaO	Al <sub>2</sub> O <sub>3</sub>	Others
Composition (wt %)	24.4	26.8	28.6	0.96	1.9	0.37	0.10	0.10	6.4	1.9	2.4	2.3	3.9

**Table 5.** Industrial operation parameters in the SKS process.

Operation Parameters	SKS Plant Data
Charging speed of dry mixed concentrates (t/h)	66
Water percent in the mixed concentrates (%)	10.21
Charging speed of flux (t/h)	5.277
Smelting temperature (K)	1473
Negative pressure in furnace (Pa)	50–200
Volume of pure oxygen (Nm <sup>3</sup> /h)	10,885
Volume of air (Nm <sup>3</sup> /h)	5651
Volume of O <sub>2</sub> in oxygen-enriched air (%)	73
Matte grade (%)	70
Oxygen efficiency (%)	99

The industrial data of matte and slag compositions as compared with the calculated data by SKSSIM are shown in Table 6. The distribution ratios of the minor elements (such as Pb, Zn, As, Sb, and Bi) among the matte, slag, and gas phase are listed in Table 7.

**Table 6.** Comparison of calculated data with actual plant data of matte and slag compositions in the SKS process.

Compositions (wt %)		Cu	Fe	S	Pb	Zn	As	Sb	Bi	SiO <sub>2</sub>
Plant data	matte	70.77	5.52	20.22	1.73	1.07	0.07	0.04	0.06	0.51
	slag	3.16	42.58	0.86	0.43	2.19	0.08	0.13	0.02	25.24
This Work	matte	70.31	4.80	20.38	1.69	1.02	0.07	0.04	0.06	0.82
	slag	2.93	42.07	0.73	0.37	2.08	0.07	0.12	0.02	25.18

**Table 7.** Comparison of calculations with actual plant data of the minor elements distributions in the SKS process.

Phases	Plant Data (%)					This Work (%)				
	As	Sb	Bi	Pb	Zn	As	Sb	Bi	Pb	Zn
Matte	5.91	12.31	19.10	55.61	17.76	6.23	12.58	18.74	56.71	17.35
Slag	12.08	71.05	11.40	24.91	64.86	11.06	72.30	11.13	23.47	66.46
Gas	82.01	16.64	69.50	19.48	17.38	82.71	15.12	70.136	19.82	16.19

The above comparisons show that the agreements between SKSSIM calculated data and industrial data are excellent. Consequently, the reliability of the SKSSIM software is validated. It thus has important practical application values, and can be used to predict the element distribution trends.

### 2.3. Calculation Process

In this work, by adjusting the blow rate of pure oxygen and air in Table 5, the blow rate of total oxygen (including pure oxygen and oxygen in air) could change from 6067 Nm<sup>3</sup>/h to 12,807 Nm<sup>3</sup>/h, and the volume fraction of O<sub>2</sub> in oxygen-enriched air was fixed at 73%. Finally, the smelting result would be that the matte grade changes from 42.57% to 76.36%. In the calculation, the composition of the mixed concentrates in the furnace was fixed.

### 3. Results and Discussion

In the present study, the elements lead, zinc, arsenic, antimony, and bismuth are discussed. The distributions of the minor elements in the SKS process are compared with the Isasmelt process [22] and the Flash smelting process [23].

#### 3.1. Distribution of Lead (Pb)

Lead is of hygiene and environmental concern, and also affects the cathode copper quality. The distribution of lead in the SKS process is given in Figure 3, which is different from that in the Isasmelt process and Flash smelting process. In normal plant operational conditions of the SKS process, the lead partitioning among off-gases, slag, and matte is 19.48%, 24.91%, and 55.61%, respectively, as listed in Table 7. The calculated results are 19.82%, 23.47%, and 56.71%, which are very close to the plant data. In the SKS process, lead enters the slag phase mostly in the form of PbO. As the matte grade increases, the proportion of PbO in slag becomes larger, whereas the proportions in both off-gas and matte decrease. When the process deals with copper concentrates with high lead contents, lead can be removed by iron silica slags by increasing the matte grade or the amount of oxygen blown into the furnace.

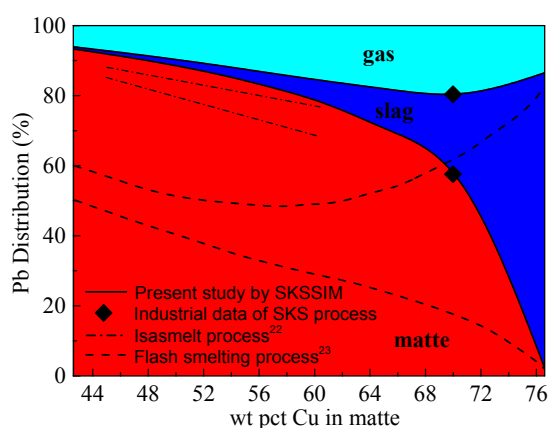


Figure 3. Lead (Pb) distribution in the SKS smelting process.

Besides thermodynamic factors, a great deal of other factors may affect the distribution of minor elements. As shown in Figure 3, with a low matte grade in the Flash smelting process, a large proportion of lead enters into gas phase, which is different from that in the SKS process or Isasmelt process. However, the distribution proportion in matte, slag, and gas phases in the SKS process is similar to that in the Isasmelt process, perhaps because they both belong to the bath smelting process. Different processes have distinctive process characteristics and operation parameters, therefore, they have different minor elements distribution behaviors.

#### 3.2. Distribution of Zinc (Zn)

Zinc is an associated element in copper sulfide minerals. The distribution of zinc among the gas, slag, and matte phases with the matte grade is presented in Figure 4. With a matte grade of 70%, most (around 64%) of the zinc reports to the slag in the form of ZnO. As the matte grade increases, the ZnO in slag becomes larger, similar to lead. However, the presence of ZnO in the copper smelting slag significantly increases the liquidus temperature in the spinel primary phase field, which further increases the slag viscosity and results in high copper losses to slag. It is difficult to recover the zinc in slag. Only a small proportion of zinc in dust can be recovered through the hydrometallurgical method. Based on the above reasons, the content of zinc in the copper concentrates should be restricted.

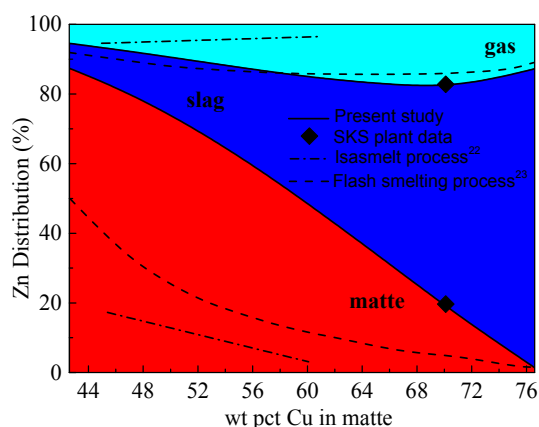


Figure 4. Zinc (Zn) distribution in the SKS smelting process.

### 3.3. Distribution of Arsenic (As)

$As_2O_3$  is a toxic substance that can cause severe environmental pollutions and serious harm to people's health. With more restrictive environment protection regulations, the industry interest is growing in the department of arsenic between various phases during the processing of copper concentrates. Figure 5 presents the variation of the calculated equilibrium distribution of arsenic among gas, slag, and matte phases as a function of matte grade. In the SKS smelting process, more than 80% of arsenic reports to the gas [24]. Its distribution among slag and matte is around 12% and 6%, respectively. Concentrating the arsenic to the gas phase is a feature of the SKS smelting process, while the Flash smelter does just the opposite, and more arsenic enters the slag. The reason for this is that the oxygen potential distributions in SKS and Flash smelting furnaces are different. This point has been explained in our previous studies [1]. With the increase of the matte grades, the proportion of arsenic reporting to the matte phase also increases. Therefore, a high matte grade is not beneficial to the removal of arsenic. When dealing with complex copper concentrates of high arsenic contents, the matte grade should be reduced appropriately.

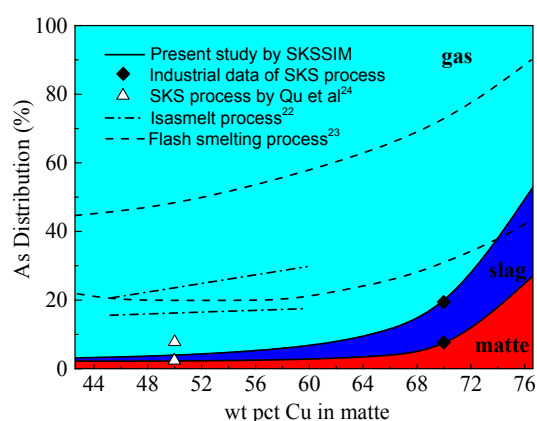


Figure 5. Arsenic (As) distribution in the SKS smelting process.

### 3.4. Distribution of Antimony (Sb)

The distribution of antimony is given in Figure 6. The variation trends of antimony distribution among gas, slag, and matte is not obvious with matte grades. Around 70% of antimony reports to the slag. Thus, it is difficult to remove antimony from matte only by adjusting the matte grade in the SKS smelting process. However, antimony can affect the physical properties of anode copper and the performance of electrolysis. So, the method of reducing the effect of antimony on copper production is

to limit the content of antimony in mixed copper concentrates before feeding into the SKS furnace by blending with raw material.

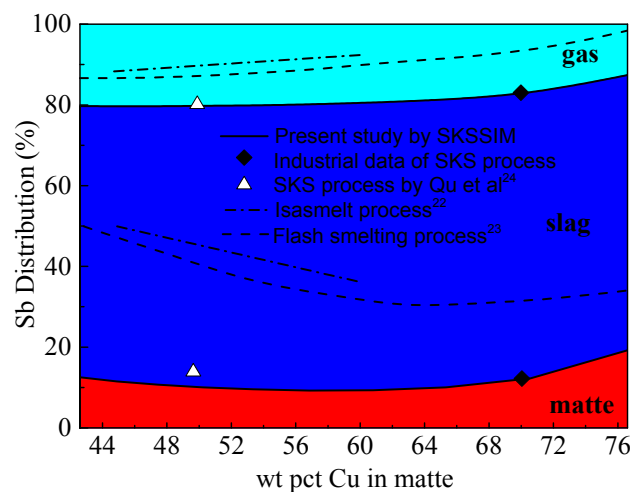


Figure 6. Antimony (Sb) distribution in the SKS smelting process.

### 3.5. Distribution of Bismuth (Bi)

The calculated distributions of bismuth are given in Figure 7 and match the industrial data well. Under normal operational conditions and with a matte grade of 70%, most bismuth reports to the gas phase, which is similar to arsenic. The proportion of bismuth reporting to the matte phase increases with the increase of matte grades, which is also similar to the variation trend of arsenic. Bismuth can increase the brittleness of anode copper and reduce its ductility, which leads to the formation of cracks in the anode copper during casting and the electrolytic process. Thus, when dealing with copper concentrates with high bismuth contents, the matte grade should be reduced.

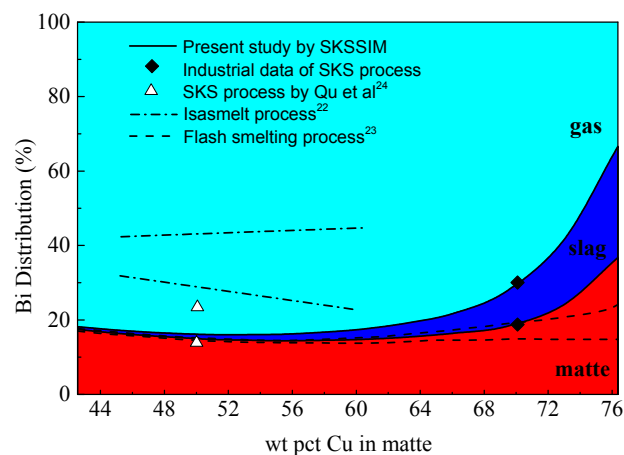


Figure 7. Bismuth (Bi) distribution in the SKS smelting process.

### 3.6. Comparison of Minor Elements Distribution

The distribution proportions of minor elements in gas, slag, and matte phases are given in Figures 8–10, respectively. Most arsenic and bismuth enter the gas phase when the matte grade is below 65%, so arsenic and bismuth could be eliminated from the SKS smelting system by a low matte grade operation. However, with a low matte grade, most lead and zinc would report to the matte phase, which increases the load of removal of impurities in the converting and refining processes.

Therefore, according to the content of impurity elements in concentrates, an optimal matte grade should be chosen.

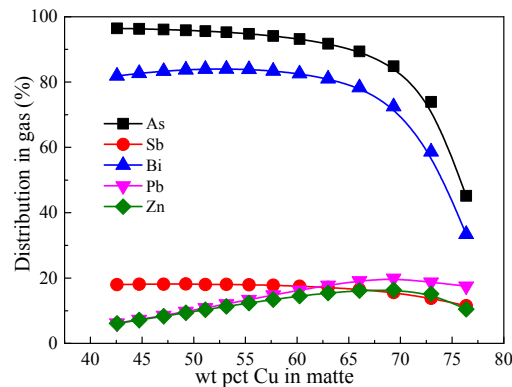


Figure 8. Minor elements distribution in gas calculated by SKSSIM.

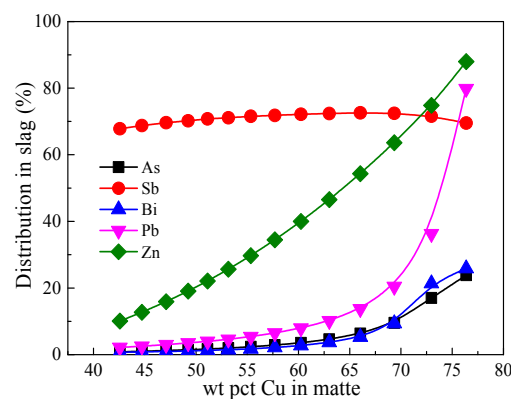


Figure 9. Minor elements distribution in slag calculated by SKSSIM.

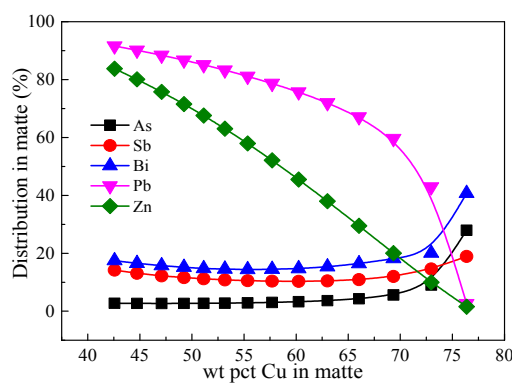


Figure 10. Minor elements distribution in matte calculated by SKSSIM.

#### 4. Conclusions

Impurities (from the ores) significantly affect the performance of copper smelting processes, and the control of minor elements is an important issue for the SKS process. Under the present operation conditions of the SKS process, the minor elements (such as Pb, Zn, As, Sb, and Bi) have different distribution behaviors among the matte, slag, and gas phases. Around 82% As and 70% Bi enters the gas phase. About 70% Sb and 64% Zn reports to the slag phase. Finally, 55% lead enters the matte phase. Based on the mechanism characteristics of the SKS process, the changing tendencies in the distribution of minor elements as a function of matte grade in the SKS process is different from that in

the Isasmelt process and Flash smelting process. Therefore, dealing with complex copper concentrates with high contents of element impurities, an optimal matte grade should be chosen to regulate the distribution of the minor elements and reduce adverse effects on the SKS process.

**Acknowledgments:** The authors would like to acknowledge the National Nature Science Foundation of China (No. 51620105013) for financial support, and Dongying Fangyuan Nonferrous Metals Co., Ltd. for providing the industrial production data.

**Author Contributions:** Xueyi Guo, Tao Jiang, and Baojun Zhao designed the research. Qinqing Wang carried out the research and wrote the paper. Xueyi Guo, Qinghua Tian, Mao Chen, and Baojun Zhao reviewed and contributed to the final manuscript.

**Conflicts of Interest:** The authors declare no conflict of interest.

## References

1. Wang, Q.M.; Guo, X.Y.; Tian, Q.H.; Chen, M.; Zhao, B.J. Reaction mechanism and distribution behavior of arsenic in the bottom blown copper smelting process. *Metals* **2017**, *7*, 302. [[CrossRef](#)]
2. Coursol, P.; Mackey, P.J.; Kapusta, J.P.T.; Valencia, N.C. Energy consumption in copper smelting: A new Asian horse in the race. *JOM* **2015**, *67*, 1066–1074. [[CrossRef](#)]
3. Li, W.F.; Zhan, J.; Fan, Y.Q.; Wei, C.; Zhang, C.F.; Hwang, J.Y. Research and industrial application of a process for direct reduction of molten high-lead smelting slag. *JOM* **2017**, *69*, 784–789. [[CrossRef](#)]
4. Chen, L.; Hao, Z.D.; Yang, T.Z.; Liu, W.F.; Zhang, D.C.; Zhang, L.; Bin, S.; Bin, W.D. A comparison study of the oxygen-rich side blow furnace and the oxygen-rich bottom blow furnace for liquid high lead slag reduction. *JOM* **2015**, *67*, 1123–1129. [[CrossRef](#)]
5. Liu, W.F.; Yang, T.Z.; Zhang, D.C.; Chen, L.; Liu, Y.F. A new pyrometallurgical process for producing antimony white from by-product of lead smelting. *JOM* **2014**, *66*, 1694–1700. [[CrossRef](#)]
6. Yan, J. Recent operation of the oxygen bottom-blowing copper smelting and continuous copper converting technologies. In Proceedings of the 9th International Copper Conference (Copper 2016), Kobe, Japan, 13–16 November 2016; pp. 1015–1030.
7. Cui, Z.X.; Wang, Z.; Wang, H.B.; Wei, C.B. Two-step copper smelting process at Dongying Fangyuan. In Proceedings of the 9th International Copper Conference (Copper 2016), Kobe, Japan, 13–16 November 2016; pp. 1043–1052.
8. Chen, M.; Cui, Z.X.; Zhao, B.J. Slag chemistry of bottom blown copper smelting furnace at Dongying Fangyuan. In Proceedings of the 6th International Symposium on High-Temperature Metallurgical Processing, Orlando, FL, USA, 15–19 March 2015; pp. 257–264.
9. Shui, L.; Cui, Z.X.; Ma, X.D.; Rhamdhani, M.A.; Nguyen, A.V.; Zhao, B.J. Mixing phenomena in a bottom blown copper smelter: A water model study. *Metall. Mater. Trans. B* **2015**, *46*, 1218–1225. [[CrossRef](#)]
10. Shui, L.; Cui, Z.X.; Ma, X.D.; Rhamdhani, M.A.; Nguyen, A.V.; Zhao, B.J. Understanding of bath surface wave in bottom blown copper smelting furnace. *Metall. Mater. Trans. B* **2016**, *47*, 135–144. [[CrossRef](#)]
11. Liu, H.Q.; Cui, Z.X.; Chen, M.; Zhao, B.J. Phase equilibrium study of ZnO–“FeO”–SiO<sub>2</sub> system at fixed P<sub>O<sub>2</sub></sub> 10<sup>−8</sup> atm. *Metall. Mater. Trans. B* **2016**, *47*, 164–177. [[CrossRef](#)]
12. Liu, H.Q.; Cui, Z.X.; Chen, M.; Zhao, B.J. Phase equilibria study of the ZnO–“FeO”–SiO<sub>2</sub>–Al<sub>2</sub>O<sub>3</sub> system at P<sub>O<sub>2</sub></sub> 10<sup>−8</sup> atm. *Metall. Mater. Trans. B* **2016**, *47*, 1113–1123. [[CrossRef](#)]
13. Zhang, Z.Y.; Chen, Z.; Yan, H.J.; Liu, F.K.; Liu, L.; Cui, Z.X.; Shen, D.B. Numerical simulation of gas-liquid multi-phase flows in oxygen enriched bottom-blown furnace. *Chin. J. Nonferr. Met.* **2012**, *22*, 1826–1834. (In Chinese)
14. Yan, H.J.; Liu, F.K.; Zhang, Z.Y.; Gao, Q.; Liu, L.; Cui, Z.X.; Shen, D.B. Influence of lance arrangement on bottom-blowing bath smelting process. *Chin. J. Nonferr. Met.* **2012**, *22*, 2393–2400. (In Chinese)
15. Guo, X.Y.; Wang, Q.M.; Tian, Q.H.; Zhang, Y.Z. Mechanism and multiphase interface behavior of copper sulfide concentrate smelting in oxygen-enriched bottom blowing furnace. *Nonferr. Met. Sci. Eng.* **2014**, *5*, 28–34. (In Chinese)
16. Guo, X.Y.; Wang, Q.M.; Tian, Q.H.; Zhao, B.J. Performance analysis and optimization of oxygen bottom blowing copper smelting process. *Chin. J. Nonferr. Met.* **2016**, *26*, 689–698. (In Chinese)
17. Liao, L.L.; Wang, Q.M.; Tian, Q.H.; Guo, X.Y. Multiphase equilibrium modeling study on the oxygen bottom blowing copper smelting (SKS) process. In Proceedings of the 9th International Copper Conference (Copper 2016), Kobe, Japan, 13–16 November 2016; pp. 1252–1264.

18. Wu, W. Mathematical Model Research and System Development of Multiphase Equilibrium in Copper Flash Smelting. Master's Thesis, Jiangxi University of Science and Technology, Ganzhou, China, June 2007. (In Chinese)
19. Shimpo, R.; Goto, S.; Ogawa, O. An improved computer program for equilibrium calculations. *Metall. Trans. A* **1993**, *24*, 1882–1889. [[CrossRef](#)]
20. Tan, P.; Zhang, C. Computer model of copper smelting process and distribution behaviors of accessory elements. *J. Cent. South Univ. Technol.* **1997**, *4*, 36–41. [[CrossRef](#)]
21. Chaubal, P.C.; Sohn, H.Y.; George, D.B.; Bailey, L.K. Mathematical modeling of minor-element behavior in flash smelting of copper concentrates and flash converting of copper mattes. *Metall. Trans. B* **1989**, *20*, 39–51. [[CrossRef](#)]
22. Nagamori, M.; Errington, W.J.; Mackey, P.J.; Poggi, D. Thermodynamic simulation model of the isasmelt process for copper matte. *Metall. Mater. Trans. B* **1994**, *25*, 839–859. [[CrossRef](#)]
23. Wang, C.; Zhang, C.F. Study on choosing the best grade matte copper smelting process. *World Nonferr. Met.* **2016**, *9*, 21–22. (In Chinese)
24. Qu, S.L.; Dong, Z.Q.; Chen, T. Distribution of minor elements in complex copper concentrates in oxygen-enriched bottom blown smelting process. *China Nonferr. Metall.* **2016**, *3*, 22–24. (In Chinese)



© 2017 by the authors. Licensee MDPI, Basel, Switzerland. This article is an open access article distributed under the terms and conditions of the Creative Commons Attribution (CC BY) license (<http://creativecommons.org/licenses/by/4.0/>).